EurJIC
European Journal of Inorganic Chemistry

Full Papers
doi.org/10.1002/ejic.202100237

Chemistry Europe
European Chemical Societies Publishing

Trimethylsilyl Pseudohalide Adducts of $GaCl_3$ and $B(C_6F_5)_3$

Kevin Bläsing,[a] Jonas Bresien,[a] Steffen Maurer,[a] Axel Schulz,*[a, b] and Alexander Villinger[a]

Me_3Si–X (X=CN, N_3, OCN, and SCN) was treated with the Lewis acids $GaCl_3$ and $B(C_6F_5)_3$ in toluene yielding the desired adducts Me_3Si–X→$GaCl_3$ and Me_3Si–X→$B(C_6F_5)_3$. All synthesized adducts were isolated and completely characterized including single crystal structure elucidations. The different structures, thermodynamics of formation and charge transfer effects are discussed on the basis of experimental and theoretical data.

Introduction

Adducts, also known as donor-acceptor complexes, are formed when a Lewis acid (electron acceptor, LA) forms a bond with a Lewis base (electron donator, LB).[1,2] Such donor-acceptor molecular complexes (LB→LA) can either be formed by a σ- or π-bond,[3–8] which is often called a dative bond.[9] Lewis acids and bases as well as their LB→LA complexes play a vital role in catalysis,[10–12] FLP chemistry,[13] chemical vapor decomposition,[11] stabilization of labile Lewis acidic or basic fragments,[14–16] structural chemistry[17–19] as well as formation of weakly coordinating anions.[20–23] Amongst many other Lewis acids,[10–13,24–26] $GaCl_3$[27–33] and $B(C_6F_5)_3$[34–40] have been used in main group chemistry in the last decades. In recent years, we have frequently used $GaCl_3$ as Lewis acid for the generation of reactive cations by chloride abstraction[41–49] and in $GaCl_3$-assisted [3+2] cycloaddition reactions yielding phosphorus-nitrogen heterocycles.[50–53] $B(C_6F_5)_3$-adducts have been utilized in our group to stabilize highly labile pseudohalide entities, such as a HCN dimer (Scheme 1**A**), HN_3 (Scheme 1**B**) and HNSO (Scheme 1**C**).[15,16,54]

As $[Me_3Si]^+$ can be considered a large proton,[55–57] we were interested in synthesizing $GaCl_3$ and $B(C_6F_5)_3$ adducts of Me_3Si–X (X = pseudohalogen) to study their structure, connectivity and bonding depending on the used Lewis acid and the pseudohalogen. There are already two reports describing the synthesis and structure of Me_3Si–N_3→$GaCl_3$ and Me_3Si–CN→$GaCl_3$.[32,58] Here we report on the synthesis and structure of the hitherto unknown Me_3Si–X→LA adducts (LA=$GaCl_3$ and $B(C_6F_5)_3$; X=CN, N_3, OCN, and SCN).

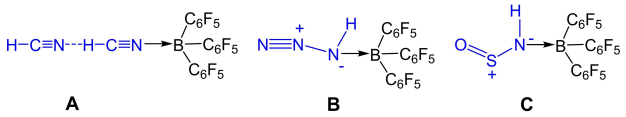

Scheme 1. Stabilization of labile pseudo halide acids by adduct formation.[15,16,54]

Results and Discussion

Synthesis

We started this project with the synthesis of the starting materials Me_3Si–X and $B(C_6F_5)_3$ (see Supporting Information). While Me_3SiCN was purchased and distilled prior to use, all other Me_3Si–X compounds were synthesized utilizing modified literature procedures.[14,59]

$B(C_6F_5)_3$ adducts

Except for X=NCO, synthesis of $B(C_6F_5)_3$ adducts Me_3Si–X→$B(C_6F_5)_3$ was achieved by addition of pure liquid Me_3Si–X to a degassed suspension of $B(C_6F_5)_3$ in toluene (X=CN, N_3) or by using an excess of Me_3Si–X without further solvent (X=NCS, Scheme 2). The suspensions at the beginning became clear after gentle heating. Colorless single crystals suitable for X-ray structure elucidation were grown by cooling utilizing different procedures (See Supporting Information). The yields range between 92 and 22% [92% (CN), 71% (N3), 22% (NCS)]. All $B(C_6F_5)_3$ adducts are moisture sensitive and melt between 108 (X=NCS) and 155 °C (CN) without decomposition. Even the Me_3Si–N_3 adduct melts without decomposition at 120 °C and decomposes above 189 °C. Notably, it was impossible to obtain the adduct Me_3S–NCO→$B(C_6F_5)_3$ since there was no reaction between the borane and Me_3Si–NCO according to solution NMR data in accord with computational results (see below).

The attempted formation of diadducts of the type Me_2Si-$[X→B(C_6F_5)_3]_2$ also failed, except for X=CN. For this purpose, Me_2SiX_2 was reacted with two equivalents of the borane in toluene, which should lead to the formation of the diadduct if possible. A yellow solution was obtained, which, however, only led to crystallization of the diadduct in the case of X=CN (a few crystals) when such a solution was cooled down in the

[a] *Dr. K. Bläsing, Dr. J. Bresien, S. Maurer, Prof. Dr. A. Schulz, Dr. A. Villinger*
Anorganische Chemie, Institut für Chemie
Universität Rostock
A.-Einstein-Str. 3a, 18059 Rostock, Germany
E-mail: axel.schulz@uni-rostock.de
[b] *Prof. Dr. A. Schulz*
Materialdesign
Leibniz-Institut für Katalyse an der Universität Rostock
A.-Einstein-Str. 29a, 18059 Rostock, Germany

Supporting information for this article is available on the WWW under https://doi.org/10.1002/ejic.202100237

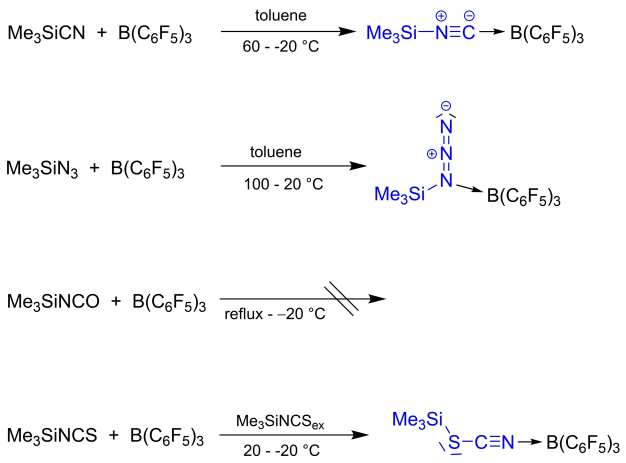

Scheme 2. Synthesis of $Me_3Si–X→B(C_6F_5)_3$ adducts (X=CN, N_3, NCO, and NCS).

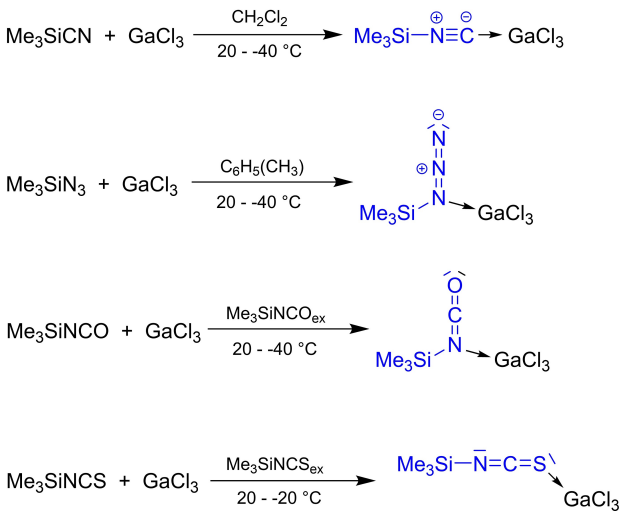

Scheme 3. Synthesis of $Me_3Si–X→GaCl_3$ adducts (X=CN, N_3, NCO, and NCS).

Table 1. Selected NMR data of the starting materials and all isolated adducts. Assignment of the isomers was carried out on the basis of computations in combination with the X-ray structure studies (See Figures 1–3, Table S12).

Compound	^{1}H	^{11}B	$^{14}N\{^{1}H\}$	^{29}Si
$B(C_6F_5)_3$		59.8		
$Me_2Si(CN)_2$	0.65	–	−79.0	−36.6
Me_3SiCN	0.98	–	−88.0	−11.2
$Me_3SiNC→B(C_6F_5)_3$	0.56	−22.0	−192.9	25.4
$Me_3SiNC→GaCl_3$	−0.28	–	[a]	30.2
Me_3SiN_3	0.29		−321.5$^{\alpha}$	16.3
			−145.4$^{\beta}$	
			−209.3$^{\gamma}$	
$Me_3SiN_3→B(C_6F_5)_3$ (1,1 isomer)	0.34	20.7	−323.3$^{\alpha}$	32.8
			−172.1$^{\beta}$	
			−143.5$^{\gamma}$	
$Me_3SiN_3→GaCl_3$ (1,1 isomer)	0.01	–	[b]	38.7
Me_3SiNCO	0.28	–	−344.2	4.3
$Me_2Si(NCO)_2$	0.31	–	−344.2	−18.2
$Me_3SiNCO→GaCl_3$ (1,1 isomer)	−0.17	–	−325.6	21.4
Me_3SiNCS	0.31	–	−261.2	6.0
$Me_2Si(NCS)_2$	0.53	–	−268.8	−22.3
$Me_3SiSCN→B(C_6F_5)_3$ (1,3 isomer)	0.60	−10.7	-	20.7
$Me_3SiNCS→GaCl_3$ (1,3 isomer)	−0.09	–	−223.1	22.8

[a] Values not given in ref. [58] [b] Not reported in ref. [32]

refrigerator. For X=OCN and SCN, however, no reaction was observed according to NMR data.

Especially, ^{11}B NMR studies are particularly well suited to visualize adduct formation in solution, since there is a very large shift in the ^{11}B resonance of the $B(C_6F_5)_3$ moiety when the adduct is formed (Table 1, $\Delta[\delta^{11}B]_{sm\text{-}adduct}$ = 81.8 (X=CN), 80.5 (N_3), and 70.5 ppm (NCS); sm = starting material).

$GaCl_3$ adducts

To synthesize $GaCl_3$ adducts of $Me_3Si–X$, gallium trichloride was either dissolved in CH_2Cl_2 (X=CN, SCN), toluene ($X=N_3$) or in an excess of pseudohalogenotrimethylsilane (X=NCO) resulting always in a slightly yellow solution (Scheme 3). Upon addition of $Me_3Si–X$, the solution became colorless within a few seconds and colorless single crystals suitable for X-ray structure elucidation were grown by cooling the solution (see Supporting Information). The crystals were rather unstable and often decomposed within a few minutes at ambient temperatures, a feature that has already been addressed by Kouvetakis et al. for $X=N_3$. Here, decomposition starts with the elimination of $Me_3Si–Cl$ along with the formation of $Cl_2Ga–X$.[32] Kouvetakis et al. prepared $Me_3SiN_3→GaCl_3$ by adding Me_3SiN_3 to a frozen solution of $GaCl_3$ at −196 °C, while we found that it is not necessary to work at very low temperatures. We added Me_3SiN_3 at −40 °C and allowed the solution to warm up to ambient temperatures. Crystals were obtained by slowly cooling down to −20 °C overnight.

Also, ^{29}Si NMR spectroscopy can be used to follow adduct formation in solution for both $GaCl_3$ as well as $B(C_6F_5)_3$ adduct formation (Table 1, $\Delta[\delta^{29}Si]_{sm\text{-}GaCl3\text{-}adduct}$ = −41.4 (X=CN), −22.4 (N_3), −17.1 (NCO), and −16.8 ppm (NCS)). However, in case of the $GaCl_3$ adducts this shift is slightly larger compared to those upon $B(C_6F_5)_3$ adduct formation (cf. $\Delta[\delta^{29}Si]_{sm\text{-}B(C6F5)3\text{-}adduct}$ = −36.6 (X=CN), −16.5 (N_3), and −14.7 ppm (NCS)).

Structure

X-ray quality crystals were selected in Fomblin YR-1800 perfluoroether (Alfa Aesar) under a stream of cooled nitrogen. The samples were cooled to 123(2) K during measurement. The single crystal X-ray structures were determined of the mono-adduct $Me_3Si–X→B(C_6F_5)_3$, X=CN, N_3, SCN and diadduct $Me_2Si-[CN→B(C_6F_5)_3]_2$ as well as $Me_3SiX→GaCl_3$, $X=N_3$, OCN, SCN. It should be noted that the structures of $Me_3Si–N_3→GaCl_3$ and $Me_3Si–CN→GaCl_3$ have already been published but their data will be used for comparison.[32,58] Since our structural data of $Me_3Si–N_3→GaCl_3$ are slightly different to the published ones but with better R values, we will use our data set in the discussion. Selected structural data are listed in Table 1.

While mono- as well as the diadducts of the CN species are always 1,2-isomers (Figure 1) with the N atom attached to the Si atom, the azide adducts feature always the 1,1-isomer (Figure 2). For X=OCN, also the 1,1-isomer with the N attached to the Si/Ga was found for the $GaCl_3$ adduct. Only the 1,3-isomers were observed for X=SCN both for the $B(C_6F_5)_3$ and $GaCl_3$ adduct, however, with the Ga attached to the sulfur atom and the borane linked to the nitrogen atom (Figure 3). See Table 2 for selected structural data.

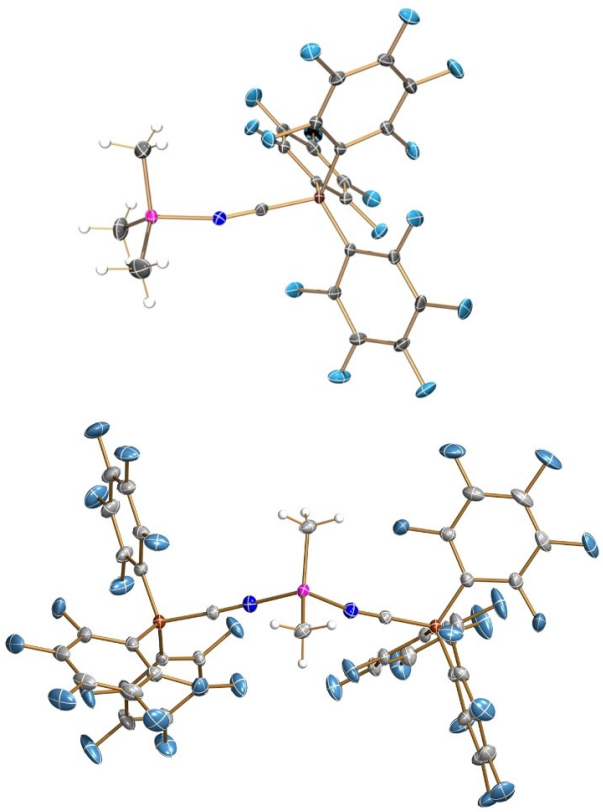

Figure 1. ORTEP representations of $Me_3SiNC{\rightarrow}B(C_6F_5)_3$ (1,2 isomer) and $Me_2Si[NC{\rightarrow}B(C_6F_5)_3]_2$ in the crystal (selected structural data are listed in Table 2). Color code: B brown, C gray, Si violet, F light blue, N blue and H white.

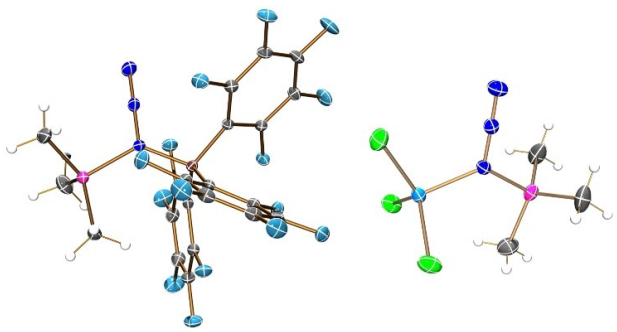

Figure 2. ORTEP representation of $Me_3SiN_3{\rightarrow}B(C_6F_5)_3$ (1,1 isomer) and $Me_3SiN_3{\rightarrow}GaCl_3$ (1,1 isomer) in the crystal (selected structural data are listed in Table 2). Color code: B brown, C gray, Si violet, F light blue, N blue, Ga turquoise, Cl, green and H white.

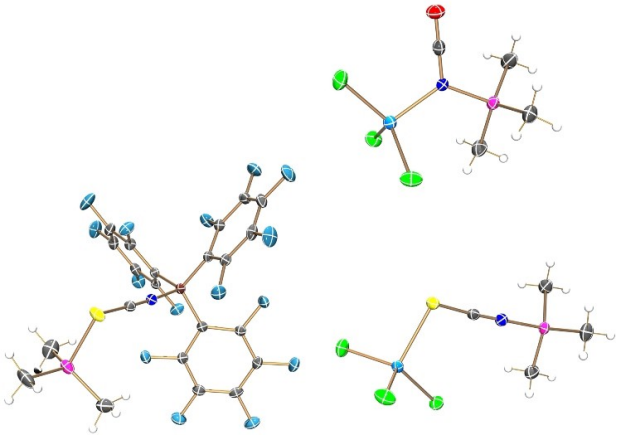

Figure 3. ORTEP representations of $Me_3Si(NCO){\rightarrow}GaCl_3$ (1,1 isomer, top); bottom: $Me_3SiNCS{\rightarrow}B(C_6F_5)_3$ (1,3 isomer) and $Me_3SiNCS{\rightarrow}GaCl_3$ (1,3 isomer) in the crystal (selected structural data are listed in Table 2). Color code: B brown, C gray, Si violet, F light blue, N blue, S yellow, Ga turquoise, Cl, green and H white.

A closer look at the structural data shows that the B–C and B–N donor-acceptor bonds (d(B–C) = 1.610–1.617, d(B–N) = 1.587–1.648 Å) are slightly longer than a classical B–C and B–N covalent bond (cf. Σr_{cov}(B–C) = 1.60, Σr_{cov}(B–C) = 1.56 Å).[60] The same applies to the Ga–C and G–N bonds (d(Ga–C) = 2.029(4), d(Ga–N) = 1.999(2), Σr_{cov}(Ga–C) = 1.99, Σr_{cov}(Ga–N) = 1.95 Å).[60] Interestingly, the B–N bond length in the 1,3-isomer of $Me_3Si{-}SCN{\rightarrow}B(C_6F_5)_3$ is significantly shorter (1.587(2) Å) than that in the 1,1-isomer of $Me_3Si{-}N_3{\rightarrow}B(C_6F_5)_3$ (1.648(2) Å). Furthermore, the CN bonds in all three cyanido-adducts are still in the range of a typical CN triple bond (1.141–1.155 Å, Σr_{cov}(C≡N) = 1.14 Å), while in the OCN adduct these are significantly longer with 1.229(4) Å and are in the range of CN double bond (Σr_{cov}(C=N) = 1.29 Å). In contrast the C–O bond is rather short with 1.153(4) Å (cf. Σr_{cov}(C=O) = 1.24 Å, Σr_{cov}(C≡O) = 1.13 Å).[60]

In the azides, it is noticeable that there are two clearly distinguishable N–N bonds. A rather long one was found for the N atom that forms the dative bond with the respective Lewis acid ($d(N_\alpha{-}N_\beta)$: 1.259(1)–1.261(2) Å, cf. (Σr_{cov}(N=N) = 1.20 Å), while the terminal N atom has a significantly shorter $N_\beta{-}N_\gamma$ bond within the N_3 unit with 1.116(2)–1.117(2) Å (Σr_{cov}(N≡N) = 1.08 Å), which is close to the distance for a triple bond. Hence, an N_2 molecule is pre-formed in the N_3 adducts.

The rhodanide complexes show a clear difference in the angle to the Lewis acid (∢(C–N–B) = 176.5(2)° vs. ∢(C–S–Ga) = 97.7(1)°), which is due to the fact that in the $GaCl_3$ adduct, the $GaCl_3$ coordinates to the heavy sulfur atom, just as in the analogous OCN adduct (here to the O atom – the lighter chalcogen), whereas in the borane adduct, the boron atom is linked to the nitrogen. That is, both adducts are different in terms of coordination to the rhodanide moiety, since in the borane adduct there is formally a trimethylsilyl thiocyanate, while in the $GaCl_3$ adduct there is an isothiocyanate. Obviously, the larger borane prefers the N atom, which leads to a minimization of the Pauli repulsion in the molecule, which is

Table 2. Selected experimental bond lengths (Å) and angles (°).[a]

Compound	Si–X	X–Y	Y–Z	X/Z–LA	X–Y–Z	Si–X–Y	Y–X/Z–LA
$Me_3SiNC\rightarrow B(C_6F_5)_3$	1.822(2)	1.148(2)	–	1.617(2)	–	165.9(2)	177.8(2)
$Me_3SiNC\rightarrow GaCl_3$[b]	1.858(3)	1.141(4)	–	2.029(4)	–	180.0	180.0
$Me_2Si(NC\rightarrow B(C_6F_5)_3)_2$	1.815(2)	1.155(3)	–	1.610(3)	–	168.4(2)	176.4(2)
$Me_3SiN_3\rightarrow B(C_6F_5)_3$ (1,1 isomer)	1.874(2)	1.259(1)	1.117(2)	1.648(2)	179.6(1)	116.65(9)	129.20(7)
$Me_3SiN_3\rightarrow GaCl_3$ (1,1 isomer)	1.854(2)	1.261(2)	1.116(2)	1.999(2)	178.6(2)	116.1(2)	115.2(2)
$Me_3SiNCO\rightarrow B(C_6F_5)_3$ *not formed*	–	–	–	–	–	–	–
$Me_3SiNCO\rightarrow GaCl_3$ (1,1 isomer)	1.861(3)	1.229(4)	1.153(4)	2.019(2)	179.6(4)	119.6(2)	114.5(2)
$Me_3SiSCN\rightarrow B(C_6F_5)_3$ (1,3 isomer)	2.253(1)	1.663(2)	1.144(2)	1.587(2)	177.8(2)	97.8(1)	176.5(2)
$Me_3SiNCS\rightarrow GaCl_3$ (1,3 isomer)	1.819(2)	1.149(2)	1.644(2)	2.371(1)	176.5(2)	179.1(2)	97.7(1)

[a] X, Y, Z correspond to the α, β, γ atoms of the pseudohalogen; LA = Lewis acid, depending on the connectivity (1,1 or 1,3 isomer). [b] Taken from ref. [58]

consistent with our quantum chemical calculations (see below). Moreover, boron as element of the 2nd period prefers bonding to the N atom, also an element of the 2nd period, while the Ga atom as element of the 4th period forms the bond to the S atom.

Thermodynamics

To shed some light into the formation of the different possible adduct isomers, quantum chemical computations have been performed at the DLPNO-CCSD(T)/def2-TZVPP//PBE0-D3BJ/def2-TZVP level of theory. Selected structural parameters are listed in Tables S13–S14 and the adduct formation energies in Table 3. The most essential statement of the thermodynamic calculations in relation to the adduct formation reaction as described in Table 3 is that molecular structures in the solid state always correspond to the thermodynamically most stable isomer. For example, both $Me_3Si–NC\rightarrow LA$ adducts are favored over the $Me_3Si–CN\rightarrow LA$ complexes ($B(C_6F_5)_3$: 6.3, $GaCl_3$: 1.93 kcal mol^{-1}). In agreement with experiment, no stable $B(C_6F_5)_3$ adduct with $Me_3Si–NCO/Me_3Si–OCN$ was found as all Gibbs energies are positive. In contrast, the 1,1-$GaCl_3$ adduct of $Me_3Si–NCO$ is formed with an energy gain of $\Delta_rG^\circ = -9.41$ kcal mol^{-1}, whereas all $Me_3Si–OCN$ adducts are thermodynamically unstable with respect to dissociation. The 1,3-isomer of the $Me_3Si–NCO$ adduct is 2.02 kcal mol^{-1} less stable than the experimentally found 1,1 adduct.

For the rhodanide adducts, the situation is different. While the 1,3-$GaCl_3$ adduct of $Me_3Si–NCS$ is the most stable complex with −7.66 kcal mol^{-1}, for the $B(C_6F_5)_3$ adduct, all complexes were computed to be thermodynamically unstable with respect to adduct dissociation.

However, since it was possible to isolate 1,3-$Me_3Si–SCN\rightarrow B(C_6F_5)_3$, it can be assumed that solid state effects such as intermolecular dipole-dipole interactions result in the formation of thermodynamically stable molecules in the solid. Moreover, the Gibbs energy, $\Delta_rG^\circ = 3.48$ kcal mol^{-1}, for the formation is rather small so this can easily be compensated by intermolecular attractive effects. Experimentally, it was found that the isolated crystals are very unstable at ambient temperatures. Additionally, since we started from the $Me_3Si–NCS$ in the experiment, an isomerization process must have occurred, which afforded finally $Me_3Si–SCN\rightarrow B(C_6F_5)_3$. Again, in agreement with experiment, all azide adducts found experimentally are those computed to be the most thermodynamically stable isomers. That is, the 1,1 isomers that have a preformed N_2 unit, are 8.8 ($B(C_6F_5)_3$) and 9.92 kcal mol^{-1} ($GaCl_3$) more stable than the 1,3 isomers. Finally, a word about charge transfer (see Table S15). It was found that the stronger Lewis acid, $B(C_6F_5)_3$, in the corresponding borane adducts receives about 0.35–0.58*e* from the Me_3SiX molecule, while $GaCl_3$ receives only about half of that (0.17–0.29*e*).

Table 3. Reactions energies (DLPNO-CCSD(T)/def2-TZVPP//PBE0-D3BJ/def2-TZVP, in kcal·mol^{-1}). Formation reaction of $Me_3SiX–LS$: $Me_3Si–X + LA\rightarrow Me_3SiX\rightarrow LA$.

$Me_3SiX\rightarrow LA$	ΔE^{tot}	Δ_RH°	Δ_RG°
$Me_3SiCN\rightarrow B(C_6F_5)_3$	−22.02	−19.12	−10.09
$Me_3SiNC\rightarrow B(C_6F_5)_3$	−28.57	−25.62	−16.39
$Me_3SiCN\rightarrow GaCl_3$	−25.32	−24.45	−11.94
$Me_3SiNC\rightarrow GaCl_3$	−25.36	−23.96	−13.87
(1,1)$Me_3SiN_3\rightarrow B(C_6F_5)_3$	−21.30	−18.61	−5.96
(1,3)$Me_3SiN_3\rightarrow B(C_6F_5)_3$	−10.63	−7.96	2.85
(1,1)$Me_3SiN_3\rightarrow GaCl_3$	−27.43	−26.11	−13.62
(1,3)$Me_3SiN_3\rightarrow GaCl_3$	−16.95	−15.50	−3.71
(1,1)$Me_3SiNCO\rightarrow B(C_6F_5)_3$	−12.21	−8.44	1.43
(1,3)$Me_3SiNCO\rightarrow B(C_6F_5)_3$[a]	−9.07	−5.29	1.15
(1,1)$Me_3SiOCN\rightarrow B(C_6F_5)_3$[a]	10.35	13.72	20.09
(1,3)$Me_3SiOCN\rightarrow B(C_6F_5)_3$	−5.96	−2.33	5.34
(1,1)$Me_3SiNCO\rightarrow GaCl_3$	−21.59	−19.15	−9.41
(1,3)$Me_3SiNCO\rightarrow GaCl_3$	−18.21	−15.81	−7.39
(1,1)$Me_3SiOCN\rightarrow GaCl_3$	5.81	7.72	16.96
(1,3)$Me_3SiOCN\rightarrow GaCl_3$	−10.46	−8.23	0.65
(1,1)$Me_3SiNCS\rightarrow B(C_6F_5)_3$	−10.76	−8.26	4.13
(1,3)$Me_3SiNCS\rightarrow B(C_6F_5)_3$[a]	−10.22	−7.65	1.61
(1,1)$Me_3SiSCN\rightarrow B(C_6F_5)_3$	11.30	13.29	24.04
(1,3)$Me_3SiSCN\rightarrow B(C_6F_5)_3$	−9.41	−6.93	3.48
(1,1)$Me_3SiNCS\rightarrow GaCl_3$	−19.15	−17.96	−5.94
(1,3)$Me_3SiNCS\rightarrow GaCl_3$	−19.90	−18.66	−7.66
(1,1)$Me_3SiSCN\rightarrow GaCl_3$	0.31	1.13	12.37
(1,3)$Me_3SiSCN\rightarrow GaCl_3$	−12.81	−11.79	−0.77

[a] No stable adduct was found, only separated weakly interacting Lewis-acid Lewis-base pairs with a distance larger than the sum of the van-der-Waals radii.

Conclusion

In conclusion, we present a series of new $Me_3Si–X\rightarrow LA$ adducts (X=CN, N_3, OCN, SCN; LA=$B(C_6F_5)_3$, $GaCl_3$). We discuss exper-

imentally as well as theoretically the influence of the Lewis acid strength and the bulkiness on the formation of the different isomers. While for X≡CN both Lewis acids form the 1,2-Me_3Si–NC→LA adduct, for the azide only the 1,1-isomers were found to be the most favored isomers. In the case of the cyanate species, it was only possible to isolate the $GaCl_3$ adduct as 1,1-Me_3Si–NCO adduct, while it was impossible to produce the analogous borane adduct, in accord with theory, which predicted an endergonic process. The reaction of the heavier congener, the rhodanide, Me_3Si–NCS with both Lewis acid led to different products: While both Lewis acids form an 1,3 isomer, the connectivity, however, was different. In the case of the $GaCl_3$ complex, Me_3Si–NCS→$GaCl_3$ was formed, whereas with $B(C_6F_5)_3$ the formation of Me_3–SCN→$B(C_6F_5)_3$ was observed.

Experimental Section

Caution! Me_3Si–X (X≡CN, N_3) is highly toxic! Appropriate safety precautions (e.g. HCN detector, gas mask, low temperature) should be taken. Experimental spectra and additional crystal structure representations can be found in the Supporting Information.

General Information: All manipulations were carried out in oxygen- and moisture-free conditions in an argon atmosphere using standard Schlenk or dry-box techniques if not mentioned otherwise.

NMR spectra were obtained on a Bruker AVANCE 250, 300 or 500 MHz spectrometer and were referenced internally to the deuterated solvent ($^{13}C\{^1H\}$: CD_2Cl_2 $\delta_{ref}=53.84$ ppm, CD_3CN $\delta_{ref}=1.3$ ppm, $C_6D_5CD_3$ $\delta_{ref}=20.43$ ppm), to protic impurities in the deuterated solvent (^1H: $CHDCl_2$ $\delta_{ref}=5.32$ ppm, CHD_2CN $\delta_{ref}=1.93$ ppm, $C_6D_5CHD_2$ $\delta_{ref}=2.08$ ppm) or externally (^{11}B: $BF_3\cdot EtO_2$ $\delta_{ref}=0$ ppm, $^{14}N\{^1H\}$: CH_3NO_2 $\delta_{ref}=0$ ppm, ^{15}N: CH_3NO_2 $\delta_{ref}=0$ ppm, ^{17}O: H_2O $\delta_{ref}=0$ ppm, $^{19}F\{^1H\}$: $CFCl_3$ $\delta_{ref}=0$ ppm, ^{29}Si: $Si(CH_3)_4$ $\delta_{ref}=0$ ppm). All measurements were carried out at ambient temperature unless stated otherwise. ^{15}N NMR shifts were derived from ^1H-^{15}N HMBC NMR spectra.

Raman spectra of crystalline samples were recorded using a LabRAM HR 800 Horiba Jobin YVON Raman spectrometer equipped with an Olympus BX41 microscope with variable lenses. The samples were excited by a red laser (633 nm, 17 mW, air-cooled HeNe laser) or a green laser (532 nm, 50 mW, air-cooled, frequency-doubled Nd:YAG solid-state laser). All measurements were carried out at ambient temperature, if not stated otherwise. For some crystalline samples, a Linkam THMS600 Temperature Controlled stage was used to cool the substances during measurement.

Elemental analyses were obtained using an Elementar vario Micro cube CHNS analyzer.

Melting points (uncorrected) were determined using a Stanford Research Systems EZ Melt at a heating rate of $5\,°C\cdot min^{-1}$.

DSC analyses were carried out at a heating rate of $5\,°C\cdot min^{-1}$ using a Mettler-Toledo DSC 823e.

Mass spectra were recorded on a Thermo Electron MAT 95-XP sector field mass spectrometer using crystalline samples.

X-ray Structure Determination: X-ray quality crystals of all compounds were selected in Kel-F-oil (Riedel de Haen) at ambient temperatures. Single crystals were measured on a Bruker D8 Quest or a Bruker Apex Kappa II CCD diffractometer using graphite-monochromated Mo Kα radiation (λ = 0.71073). The structures were solved by iterative methods (*SHELXT*)[61] and refined by full-matrix least squares procedures (*SHELXL*).[62] Semi-empirical absorption corrections were applied (SADABS).[63] All non-hydrogen atoms were refined anisotropically and hydrogen atoms were included in the refinement at calculated positions using a riding model.

Syntheses of adduct complexes

Me_3SiNC–$B(C_6F_5)_3$

To a degassed suspension of tris(pentafluorophenyl)borane $B(C_6F_5)_3$ (221 mg, 0.43 mmol) in toluene (1.5 mL) cyanotrimethylsilane Me_3SiCN (54 mg, 0.54 mmol, ~72 µL) was added *via* µL-syringe. The suspension became clear within a few seconds and after a few more seconds a precipitate was observed. The precipitate was dissolved by heating the solution to 60 °C (oil bath). Colorless single crystals suitable for X-ray structure elucidation were grown by cooling the solution overnight to −20 °C (refrigerator with isopropanol bath). The supernatant is removed by syringe and discarded. The remaining crystals are dried ($1\cdot10^{-3}$ mbar) at 60 °C for 2 hours, yielding 241 mg (0.39 mmol, 92 %) of isocyanotrimethylsilane tris(pentafluorophenyl)borane adduct [Me_3SiNC–$B(C_6F_5)_3$].

$C_{22}H_9BF_{15}NSi$ ($611.19\,g\cdot mol^{-1}$): **mp**. 155 °C, >300 °C (dec.). **EA** calc. (found), %: C, 43.23 (43.73); H, 1.48 (1.51); N, 2.29 (2.41). **^1H NMR** (25 °C, CD_2Cl_2, 300.13 MHz): $\delta=0.56$ (s, 9H, CH_3, $^1J(^1H$-$^{13}C)=123$ Hz, $^2J(^1H$-$^{29}Si)=7.4$ Hz). **^{11}B NMR** (25 °C, CD_2Cl_2, 96.29 MHz): $\delta=-22.0$ (br, $NB(C_6F_5)_3$, $\Delta\nu_{1/2}=75$ Hz). **$^{13}C\{^1H\}$ NMR** (25 °C, CD_2Cl_2, 75.47 MHz): $\delta=-0.9$ (s, $SiCH_3$, $^1J(^{13}C$–$^{29}Si)=60$ Hz), 114.5 (br, *ipso*-C_6F_5), 137.9 (dm, *m*-CF, $^1J(^{13}C$–$^{19}F)=249$ Hz), 141.0 (dm, *p*-CF, $^1J(^{13}C$–$^{19}F)=251$ Hz), 145.1 (br, *C*N), 148.8 (dm, *o*-CF, $^1J(^{13}C$–$^{19}F)=245$ Hz). **$^{14}N\{^1H\}$ NMR** (25 °C, CD_2Cl_2, 36.14 MHz): $\delta=-192.9$ (br, Si–*N*C, $\Delta\nu_{1/2}=430$ Hz). **$^{19}F\{^1H\}$ NMR** (25 °C, CD_2Cl_2, 282.40 MHz): $\delta=-162.2$ (m, 6F, *m*-CF, $^1J(^{19}F$–$^{13}C)=249$ Hz), −157.3 (m, 3F, *p*-CF, $^1J(^{19}F$–$^{13}C)=251$ Hz), −133.3 (m, 6F, *o*-CF, $^1J(^{19}F$–$^{13}C)=245$ Hz). **^{29}Si INEPT NMR** (25 °C, CD_2Cl_2, 59.63 MHz): $\delta=25.4$ (dec, $SiCH_3$, $^2J(^{29}Si$–$^1H)=7.4$ Hz). **IR** (ATR, 32 Scans, 25 °C, cm^{-1})*: 2254 (m), 1645 (m), 1516 (s), 1460 (s), 1381 (m), 1286 (m), 1263 (m), 1099 (s), 1086 (m), 979 (s), 970 (s), 922 (m), 901 (m), 864 (s), 843 (s), 808 (s), 773 (m), 766 (m), 750 (m), 731 (m), 689 (m), 681 (s), 644 (m), 635 (m), 613 (m), 584 (w), 544 (m). **Raman** (633 nm, 8 mW, 15 s, 20 acc., 25 °C, cm^{-1}): 2975 (1), 2914 (2), 2254 (10), 1645 (2), 1392 (1), 1380 (1), 808 (1), 776 (1), 764 (1), 749 (1), 688 (1), 645 (3), 634 (1),628 (2), 587 (3), 582 (2), 578 (3), 544 (2), 488 (5), 457 (1), 445 (2), 392 (3),378 (1),372 (1), 355 (1), 345 (1), 283 (1), 263 (1), 241 (1), 230 (1), 216 (1). **MS** (CI^+, m/z (%)): 73 (19) $[Me_3Si]^+$, 100 (100) $[Me_3SiCNH]^+$, 172 (91) $[Me_3Si$–NC–$SiMe_3]^+$, 444 (42) $[Me_3Si$–NC–$B(C_6F_5)_2]^+$, 611 (65) $[Me_3Si$–NC–$B(C_6F_5)_3]^+$.

Me_3SiNC–$GaCl_3$

Gallium trichloride $GaCl_3$ (182 mg, 1.03 mmol) was dissolved in CH_2Cl_2 (2 mL) resulting in a slightly yellow solution. The solution became colorless within a few seconds by adding cyanotrimethylsilane Me_3SiCN (103 mg, 1.04 mmol) at −20 °C (isopropanol bath). Colorless single crystals suitable for X-ray structure elucidation were grown by cooling the solution overnight to −80 °C. The crystals were identified as Me_3SiCN–$GaCl_3$ adduct. The supernatant is removed by syringe and discarded. The remaining crystals are dried ($1\cdot10^{-3}$ mbar) at −20 °C for 20 minutes. The crystals were rather unstable and decomposed within a few minutes at ambient temperatures.

$C_4H_9SiNGaCl_3$ ($275.29\,g\cdot mol^{-1}$): **^1H NMR** (25 °C, toluene-d_8, 300.13 MHz): $\delta=-0.28$ (s), 0.21 (s). **^{29}Si INEPT NMR** (25 °C, toluene-d_8, 59.63 MHz): $\delta=30.2$ (dec, $SiCH_3$, $^2J(^{29}Si$–$^1H)=6.5$ Hz). A full set of analytical data could be found in the literature.[58]

Me_3SiN_3–$B(C_6F_5)_3$ (1,1 isomer)

To a degassed suspension of tris(pentafluorophenyl)borane B(C6F5)3 (212 mg, 0.41 mmol) in toluene (1.5 mL), azidotrimethylsilane Me3SiN3 (58 mg, 0.50 mmol, ~67 µL) was added *via* µL-syringe. The suspension became clear within a few seconds and after a few more seconds a precipitate was observed. The precipitate was dissolved by heating the solution to 100 °C (oil bath). Colorless single crystals suitable for X-ray structure elucidation were grown by cooling the solution overnight to 5 °C. The supernatant is removed by syringe and discarded. The remaining crystals are dried ($1 \cdot 10^{-3}$ mbar) at 40 °C for 30 minutes, yielding 182 mg (0.29 mmol, 71 %) of azidotrimethylsilane tris(pentafluorophenyl)borane adduct [Me3SiN3–B(C6F5)3 (1,1 isomer)].

$C_{21}H_9BF_{15}N_3Si$ (627.19 g·mol^{-1}): **mp**. 120 °C, 189 °C (dec.). **EA** calc. (found), %: C, 40.22 (39.79); H, 1.45 (1.53); N, 6.70 (6.66). **^{1}H NMR** (25 °C, CD_2Cl_2, 300.13 MHz): $\delta = 0.34$ (s, 9H, CH_3, $^1J(^1H–^{13}C) = 121.4$ Hz, $^2J(^1H–^{29}Si) = 6.9$ Hz). **^{11}B NMR** (25 °C, CD_2Cl_2, 96.29 MHz): $\delta = 20.7$ (br, $NB(C_6F_5)_3$, $\Delta\nu_{1/2} = 400$ Hz). **^{13}C{^{1}H} NMR** (25 °C, CD_2Cl_2, 75.47 MHz): $\delta = -1.4$ (s, $SiCH_3$, $^1J(^{13}C–^{29}Si) = 60$ Hz), 114.9 (br, *ipso*-C_6F_5), 137.9 (dm, *m*-*C*F, $^1J(^{13}C–^{19}F) = 252$ Hz), 142.9 (dm, *p*-*C*F, $^1J(^{13}C–^{19}F) = 256$ Hz), 148.6 (dm, *o*-*C*F, $^1J(^{13}C–^{19}F) = 246$ Hz). **^{14}N{^{1}H} NMR** (25 °C, CD_2Cl_2, 36.14 MHz): $\delta = -323.3$ (br, Si–*N*NN, $\Delta\nu_{1/2} = 2300$ Hz), $\delta = -172.1$ (br, Si–N*N*N, $\Delta\nu_{1/2} = 950$ Hz), $\delta = -143.5$ (br, Si–NN*N*, $\Delta\nu_{1/2} = 35$ Hz). **^{19}F{^{1}H} NMR** (25 °C, CD_2Cl_2, 282.40 MHz): $\delta = -162.7$ (m, 6F, *m*-*C*F, $^1J(^{19}F–^{13}C) = 252$ Hz), −151.4 (m, 3F, *p*-*C*F, $^1J(^{19}F–^{13}C) = 256$ Hz), −131.3 (m, 6F, *o*-*C*F, $^1J(^{19}F–^{13}C) = 246$ Hz). **^{29}Si INEPT NMR** (25 °C, CD_2Cl_2, 59.63 MHz): $\delta = 32.8$ (dec, $SiCH_3$, $^2J(^{29}Si–^1H) = 6.9$ Hz). **Raman** (633 nm, 8 mW, 15 s, 20 acc., 25 °C, cm^{-1}): 2987 (1), 2967 (1), 2920 (2), 2535 (1), 2163 (1), 1651 (3), 1646 (3), 1520 (1), 1385 (2), 1375 (1), 1204 (1), 875 (1), 857 (1), 839 (1), 787 (1), 774 (1), 757 (1), 747 (1), 708 (1), 682 (1), 653 (1), 636 (5), 593 (1), 579 (10), 549 (1), 490 (5), 475 (4), 446 (6), 417 (4), 405 (2), 393 (4), 376 (1), 358 (2), 347 (1), 316 (1), 306 (1), 284 (1), 243 (2), 232 (1). **MS** (CI$^+$, m/z (%)): 73 (8) $[(CH_3)_3Si]^+$, 116 (55) $[(CH_3)_3SiN_3H]^+$, 188 (100) $[(CH_3)_3Si–N_3–Si(CH_3)_3]^+$, 512 (68) $[B(C_6F_5)_3]^{\bullet+}$.

Me_3SiN_3–$GaCl_3$ (1,1 isomer)

Gallium trichloride $GaCl_3$ (180 mg, 1.02 mmol) was dissolved in toluene (1 mL) resulting in a slightly yellow solution. The solution became colorless within a few seconds by adding azidotrimethylsilane Me_3SiN_3 (132 mg, 1.15 mmol) at −40 °C (isopropanol bath). Colorless single crystals suitable for X-ray structure elucidation were grown by cooling the solution overnight from ambient temperatures to −20 °C (refrigerator with isopropanol bath). The crystals were identified as Me_3SiN_3–$GaCl_3$ adduct (1,1 isomer). The supernatant is removed by syringe and discarded. The remaining crystals are dried ($1 \cdot 10^{-3}$ mbar) at −20 °C for 20 minutes. The crystals were rather unstable and decomposed within a few minutes at ambient temperatures.

$C_3H_9SiN_3GaCl_3$ (291.29 g·mol^{-1}): **^{1}H NMR** (25 °C, Toluol-d_8, 300.13 MHz): $\delta = 0.01$ (s), 0.21 (s). **^{29}Si INEPT NMR** (25 °C, Toluol-d_8, 59.63 MHz): $\delta = 38.7$ (m, $SiCH_3$). A full set of analytical data could be found in the literature.[32]

Me_3SiNCO–$GaCl_3$ (1,1 isomer)

Gallium trichloride $GaCl_3$ (155 mg, 0.88 mmol) was dissolved in an excess of isocyanatotrimethylsilane (0.2 mL). The Lewis acid dissolved within 10 minutes at ambient temperatures. Colorless single crystals suitable for X-ray structure elucidation were grown by cooling the degassed solution overnight from ambient temperatures to −40 °C (isopropanol bath). The crystals were identified as Me_3SiNCO–$GaCl_3$ adduct (1,1 isomer). The supernatant is removed by syringe and discarded. The remaining crystals are dried ($1 \cdot 10^{-3}$ mbar) at −20 °C (isopropanol bath) for 20 minutes. The crystals were rather unstable and decomposed within a few minutes at ambient temperatures.

$C_4H_9Cl_3GaNOSi$ (291.29 g·mol^{-1}): **^{1}H NMR** (25 °C, toluene-d_8, 500.13 MHz): $\delta = -0.17$ (s, 9H, $(CH_3)_3Si$, $^1J(^1H–^{13}C) = 122$ Hz, $^2J(^1H–^{29}Si) = 7$ Hz). **^{13}C{^{1}H} NMR** (25 °C, toluene-d_8, 125.8 MHz): $\delta = -0.7$ (s, $(CH_3)_3Si$, $^1J(^{13}C–^{29}Si) = 60$ Hz), 137.1 (s, *N*CO). **^{14}N{^{1}H} NMR** (25 °C, toluene-d_8, 36.1 MHz): $\delta = -335.4$ (br, 1 N, *N*CO, $\Delta\nu_{1/2} = 430$ Hz), −325.6 (br, 1 N, *N*CO, $\Delta\nu_{1/2} = 510$ Hz). **^{15}N NMR** (25 °C, toluene-d_8, 50.7 MHz): $\delta = -327.1$ (s, *N*CO). **^{29}Si INEPT NMR** (25 °C, toluene-d_8, 99.4 MHz): $\delta = 6.0$ (dec, $(CH_3)_3SiNCO$, $^2J(^1H–^{29}Si) = 7$ Hz). **Raman** (532 nm, 13.5 mW, 10 s, 30 acc., 25 °C, cm^{-1}): 2977 (1), 2911 (5), 2326 (1), 2253 (1), 2240 (1), 1537 (1), 1460 (0), 1398 (1), 1324 (1), 1317 (6), 1258 (1), 1215 (1), 996 (1), 803 (1), 772 (1), 712 (1), 636 (2), 609 (1), 431 (1), 394 (10), 365 (5), 280 (6).

Me_3SiSCN–$B(C_6F_5)_3$ (1,3 isomer)

Tris(pentafluorophenyl)borane $B(C_6F_5)_3$ (256 mg, 0.50 mmol) was dissolved in isothiocyanotrimethylsilane Me_3SiNCS (1.02 mg, 7.75 mmol, ~1.2 mL). Colorless single crystals suitable for X-ray structure elucidation were grown by storing the degassed solution for 2 weeks at −20 °C (refrigerator). The supernatant is removed by syringe and discarded. The remaining crystals are dried ($1 \cdot 10^{-3}$ mbar) at 25 °C for 1 hour, yielding 72 mg (0.11 mmol, 22 %) of thiocyanotrimethylsilane tris(pentafluorophenyl)borane adduct [Me_3SiSCN–$B(C_6F_5)_3$ (1,3 isomer)]. The isolated crystals are rather unstable at ambient temperature. In the elemental analysis, the adduct is present in a 2 : 1 ratio with the borane. In NMR spectra the adduct is very labile, so that Me_3SiSCN–$B(C_6F_5)_3$ (1,3 isomer) and Me_3SiNC–$B(C_6F_5)_3$ can be observed, which is also indicated by a yellow coloration of the reaction solution.

$C_{22}H_9BF_{15}NSSi$ (643.26 g·mol^{-1}): **mp**. 108 °C. **EA** calc. (found), %: C, 41.41 (42.29); H, 1.01 (1.04); N, 1.56 (1.44); S, 3.57 (3.87).). **^{1}H NMR** (25 °C, CD_2Cl_2, 300.13 MHz): $\delta = 0.60$ (br, 9H, CH_3). **^{11}B NMR** (25 °C, CD_2Cl_2, 96.29 MHz): $\delta = -10.7$ (br, Me_3SiSCN–$B(C_6F_5)_3$, $\Delta\nu_{1/2} = 75$ Hz) −22.2 (br, Me_3SiCN–$B(C_6F_5)_3$, $\Delta\nu_{1/2} = 75$ Hz). **^{13}C{^{1}H} NMR** (25 °C, CD_2Cl_2, 75.47 MHz): $\delta = 0.5$ (s, $NCSiCH_3$), 1.8 (s, $NCSSiCH_3$), 114.5 (br, *ipso*-C_6F_5), 137.7 (dm, *m*-*C*F, $^1J(^{13}C–^{19}F) = 249$ Hz), 141.1 (dm, *p*-*C*F, $^1J(^{13}C–^{19}F) = 251$ Hz), 145.1 (br, *C*N), 148.4 (dm, *o*-*C*F, $^1J(^{13}C–^{19}F) = 245$ Hz). **^{19}F{^{1}H} NMR** (25 °C, CD_2Cl_2, 282.40 MHz): $\delta = -162.5$ (m, 6F, *m*-*C*F (Me_3SiNCS), $^1J(^{19}F–^{13}C) = 249$ Hz), −162.1 (m, 6F, *m*-*C*F (Me_3SiNC), $^1J(^{19}F–^{13}C) = 249$ Hz), −157.4 (m, 3F, *p*-*C*F (Me_3SiNCS), $^1J(^{19}F–^{13}C) = 251$ Hz), −157.2 (m, 3F, *p*-*C*F (Me_3SiNC), $^1J(^{19}F–^{13}C) = 251$ Hz), −133.1 (m, 6F, *o*-*C*F (Me_3SiNCS), $^1J(^{19}F–^{13}C) = 245$ Hz), −132.7 (m, 6F, *o*-*C*F (Me_3SiNC), $^1J(^{19}F–^{13}C) = 245$ Hz). **^{29}Si INEPT NMR** (25 °C, CD_2Cl_2, 59.63 MHz): $\delta = 20.7$ (dec, $CNSiCH_3$, $^2J(^{29}Si–^1H) = 7.4$ Hz), 46.7 (dec, $SCNSiCH_3$, $^2J(^{29}Si–^1H) = 7.4$ Hz). **IR** (ATR, 32 scans, 25 °C, cm^{-1})*: 569 (m), 577 (m), 592 (m), 619 (m), 633 (m), 665 (m), 679 (m), 739 (m), 773 (m), 798 (m), 835 (m), 854 (m), 968 (s), 1097 (s), 1259 (m), 1284 (m), 1381 (m), 1456 (vs), 1518 (s), 1601 (m), 1645 (m), 2015 (w), 2056 (w), 2094 (m), 2154 (w), 2173 (w), 2187 (w), 2197 (w), 2212 (w), 2245 (w), 2966 (w), 3304 (w), 3552 (w), 3676 (w). **Raman** (633 nm, 8 mW, 15 s, 20 acc., 25 °C, cm^{-1}): 2975 (1), 2913 (1), 2541 (1), 2245 (10), 2214 (1), 2197 (1), 2196 (1), 1649 (1), 1521 (1), 1385 (1), 1315 (1), 1274 (1), 1262 (1), 1115 (1), 951 (1), 832 (1), 774 (1), 763 (1), 741 (1), 711 (1), 681 (1), 666 (1), 624 (3), 591 (1), 578 (4), 511 (1), 491 (5), 473 (1), 447 (3), 411 (2), 391 (3), 373 (2), 355 (1), 351 (1), 321 (1), 294 (1), 285 (1), 276 (1), 261 (1), 247 (1), 234 (1), 211 (1). **MS** (CI$^+$, m/z (%)): 106 (7) $[Me_3Si–S–H]^+$, 132 (100) $[Me_3Si–SCN–H]^+$, 163 (10) $[Me_3Si–NCS–SiMe_2]^+$,204 (52) $[Me_3Si–NCS–SiMe_3]^+$, 262 (17) $[(Me_3Si)_2–NCS–C(CH_3)_3]^+$, 550 (7) $[(Me_3Si)_2SCN–BH(C_6F_5)_2]^+$.

* measured under non-inert conditions, hydrolysis (signals $>3300\ cm^{-1}$)

Me_3SiNCS–$GaCl_3$ (1,3 isomer)

Gallium trichloride $GaCl_3$ (180 mg, 1.05 mmol) was dissolved in CH_2Cl_2 (0.5 mL). The degassed solution was cooled to −20 °C (isopropanol bath) and isothiocyanotrimethylsilane (135 mg, 1.03 mmol) was added *via* µL-syringe. Colorless single crystals suitable for X-ray structure elucidation were grown by cooling the degassed solution overnight from −20 °C to −40 °C (isopropanol bath). The crystals were identified as isothiocyanotrimethylsilane gallium trichloride adduct Me_3SiNCS–$GaCl_3$ (1,3 isomer). The supernatant is removed by syringe and discarded. The remaining crystals are dried ($1\cdot10^{-3}$ mbar) −20 °C for 20 minutes. The crystals were rather unstable and decomposed within a few minutes at temperatures about 0 °C.

$C_4H_9Cl_3GaNSSi$ (307.36 $g\cdot mol^{-1}$): **^{1}H NMR** (25 °C, toluene-d_8, 500.13 MHz): $\delta=-0.15$ (s, 9H, $(CH_3)_3$Si–N–Ga), −0.09 (s, 9H, $(CH_3)_3$Si–NCS–Ga). **^{13}C{^{1}H} NMR** (25 °C, toluene-d_8, 125.8 MHz): $\delta=-1.5$ (s, $(CH_3)_3$Si, $^1J(^{13}C–^{29}Si)=60$ Hz), 132.3 (s, *N*CS). **^{14}N{^{1}H} NMR** (25 °C, toluene -d_8, 36.1 MHz): $\delta=-223.1$ (s, 1 N, *N*CS, $\Delta\nu_{1/2}=90$ Hz), −204.4 (br, 1 N, *N*CS, $\Delta\nu_{1/2}=360$ Hz). **^{29}Si INEPT NMR** (25 °C, toluene -d_8, 99.4 MHz): $\delta=22.8$ (dec, $(CH_3)_3$*Si*NCS, $^2J(^1H–^{29}Si)=7$ Hz). **Raman** (532 nm, 13.5 mW, 10 s, 20 acc., 25 °C, cm^{-1}): 2969 (2), 2906 (8), 2782 (1), 2174 (8), 1421 (1), 1391 (1), 1275 (1), 1264 (1), 867 (1), 772 (1), 713 (0), 631 (7), 492 (1), 389 (2), 356 (10), 296 (2), 266 (2), 252 (2), 210 (2).

Deposition Numbers 1976402 [for Me_3SiNC–$B(C_6F_5)_3$], 1976403 [for Me_3SiNCO–$GaCl_3$ (1,1 isomer)], 1976404 [for Me_3SiNCS–$GaCl_3$ (1,3 isomer)], 1976405 [for Me_3SiSCN–$B(C_6F_5)_3$ (1,3 isomer)], 1886223 [for $Me_3SiN_3\rightarrow B(C_6F_5)_3$ (1,1 isomer)], and 1251213 [for $Me_3SiN_3\rightarrow GaCl_3$ (1,1 isomer)] contain the supplementary crystallographic data for this paper. These data are provided free of charge by the joint Cambridge Crystallographic Data Centre and Fachinformationszentrum Karlsruhe Access Structures service www.ccdc.cam.ac.uk/structures.

Acknowledgements

The "Deutsche Forschungsgemeinschaft" (DFG SCHU 1170/12-1) is acknowledged for financial support (K.B.). We also thank the University of Rostock for access to the cluster computer and especially Malte Willert for technical support. Open access funding enabled and organized by Projekt DEAL.

Conflict of Interest

The authors declare no conflict of interest.

Keywords: Adducts · Azides · Cyanates · Cyanides · Pseudohalogens · Rhodanides

[1] M. Nič, J. Jirát, B. Košata, A. Jenkins, A. McNaught, Eds., *IUPAC Compendium of Chemical Terminology*, IUPAC, Research Triagle Park, NC, NC, **1994**.
[2] P. Muller, *Pure Appl. Chem.* **1994**, *66*, 1077–1184.
[3] G. Frenking, M. Hermann, in *Chem. Bond I*, Springer International Publishing Switzerland, **2016**, pp. 131–156.
[4] K.-A. Østby, G. Gundersen, A. Haaland, H. Nöth, *Dalton Trans.* **2005**, 2284–91.
[5] C. Loschen, K. Voigt, J. Frunzke, A. Diefenbach, M. Diedenhofen, G. Frenking, *Z. Anorg. Allg. Chem.* **2002**, *628*, 1294.
[6] M. F. Ibad, P. Langer, A. Schulz, A. Villinger, *J. Am. Chem. Soc.* **2011**, *133*, 21016–21027.
[7] M. F. Ibad, A. Schulz, A. Villinger, *Organometallics* **2019**, *38*, 1445–1458.
[8] M. F. Ibad, A. Schulz, A. Villinger, *Organometallics* **2015**, *34*, 3893–3901.
[9] A. Haaland, *Angew. Chem. Int. Ed.* **2006**, *101*, 1017–1032.
[10] W. E. Piers, T. Chivers, *Chem. Soc. Rev.* **1997**, *26*, 345–354.
[11] E. I. Davydova, T. N. Sevastianova, A. V. Suvorov, A. Y. Timoshkin, *Coord. Chem. Rev.* **2010**, *254*, 2031–2077.
[12] F. Focante, P. Mercandelli, A. Sironi, L. Resconi, *Coord. Chem. Rev.* **2006**, *250*, 170–188.
[13] D. W. Stephan, G. Erker, *Angew. Chem. Int. Ed.* **2010**, *49*, 46–76; *Angew. Chem.* **2010**, *122*, 50–81.
[14] M. Lehmann, A. Schulz, A. Villinger, *Angew. Chem. Int. Ed.* **2009**, *48*, 7444–7447; *Angew. Chem.* **2009**, *121*, 7580–7583.
[15] K. Bläsing, J. Bresien, R. Labbow, D. Michalik, A. Schulz, M. Thomas, A. Villinger, *Angew. Chem. Int. Ed.* **2019**, *58*, 6540–6544; *Angew. Chem.* **2019**, *131*, 6610–6615.
[16] K. Bläsing, J. Bresien, R. Labbow, A. Schulz, A. Villinger, *Angew. Chem. Int. Ed.* **2018**, *57*, 9170–9175; *Angew. Chem.* **2018**, *130*, 9311–9316.
[17] C. Aubauer, E. Irran, C. Keck, T. M. Klapötke, W. Schnick, A. Schulz, J. Senker, *Phosphorus Sulfur Silicon Relat. Elem.* **2001**, *169*, 189–192.
[18] C. Aubauer, E. Irran, T. M. Klapötke, W. Schnick, A. Schulz, J. Senker, *Inorg. Chem.* **2001**, *40*, 4956–4965.
[19] C. Hubrich, D. Michalik, A. Schulz, A. Villinger, *Z. Anorg. Allg. Chem.* **2008**, *634*, 1403–1408.
[20] I. Krossing, I. Raabe, *Angew. Chem. Int. Ed.* **2004**, *43*, 2066–90; *Angew. Chem.* **2004**, *116*, 2116–2142.
[21] T. A. Engesser, M. R. Lichtenthaler, M. Schleep, I. Krossing, *Chem. Soc. Rev.* **2016**, *45*, 789–899.
[22] A. Bernsdorf, H. Brand, R. Hellmann, M. Köckerling, A. Schulz, A. Villinger, K. Voss, *J. Am. Chem. Soc.* **2009**, *131*, 8958–8970.
[23] M. Karsch, H. Lund, A. Schulz, A. Villinger, K. Voss, *Eur. J. Inorg. Chem.* **2012**, *2012*, 5542–5553.
[24] G. He, O. Shynkaruk, M. W. Lui, E. Rivard, *Chem. Rev.* **2014**, *114*, 7815–7880.
[25] H. Yamamoto, *Lewis Acid Reagents – A Practical Approach*, Oxford, **2003**.
[26] S. Schulz, *Coord. Chem. Rev.* **2001**, *215*, 1–37.
[27] G. L'abbe, *Chem. Rev.* **1969**, *69*, 345–363.
[28] N. Burford, J. A. C. Clyburne, P. K. Bakshi, T. S. Cameron, *Organometallics* **1995**, *14*, 1578–1585.
[29] F. Reiß, A. Schulz, A. Villinger, *Chem. Eur. J.* **2014**, *20*, 11800–11811.
[30] W. Baumann, D. Michalik, F. Reiß, A. Schulz, A. Villinger, *Angew. Chem. Int. Ed.* **2014**, *53*, 3250–3253; *Angew. Chem.* **2014**, *126*, 3314–3318.
[31] V. S. Korotkov, O. V. Larionov, A. Hofmeister, J. Magull, A. de Meijere, *J. Org. Chem.* **2007**, *72*, 7504–10.
[32] J. Kouvetakis, J. McMurran, P. Matsunaga, M. O'Keeffe, J. L. Hubbard, *Inorg. Chem.* **1997**, *36*, 1792–1797.
[33] H. Brand, A. Schulz, A. Villinger, *Z. Anorg. Allg. Chem.* **2007**, *633*, 22–35.
[34] V. D. Aftandilian, H. C. Miller, G. W. Parshall, E. L. Muetterties, *Inorg. Chem.* **1962**, *1*, 734–737.
[35] A. A. Danopoulos, J. R. Galsworthy, M. L. H. Green, L. H. Doerrer, S. Cafferkey, M. B. Hursthouse, *Chem. Commun.* **1998**, 2529–2560.
[36] I. C. Vei, S. I. Pascu, M. L. H. Green, J. C. Green, R. E. Schilling, G. D. W. Anderson, L. H. Rees, *Dalton Trans.* **2003**, 2550–2557.
[37] G. Dierker, J. Ugolotti, G. Kehr, R. Fröhlich, G. Erker, *Adv. Synth. Catal.* **2009**, *351*, 1080–1088.
[38] X. Wang, P. P. Power, *Angew. Chem. Int. Ed.* **2011**, *50*, 10965–10968; *Angew. Chem.* **2011**, *123*, 11157–11160.
[39] M. M. Hansmann, R. L. Melen, F. Rominger, A. S. K. Hashmi, D. W. Stephan, *J. Am. Chem. Soc.* **2014**, *136*, 777–782.
[40] R. Kather, E. Rychagova, P. Sanz Camacho, S. E. Ashbrook, J. D. Woollins, L. Robben, E. Lork, S. Ketkov, J. Beckmann, *Chem. Commun.* **2016**, *52*, 10992–10995.
[41] A. Schulz, A. Villinger, *Inorg. Chem.* **2009**, *48*, 7359–7367.
[42] M. Lehmann, A. Schulz, A. Villinger, *Angew. Chem. Int. Ed.* **2012**, *51*, 8087–8091; *Angew. Chem.* **2012**, *124*, 8211–8215.
[43] C. Hering, M. Hertrich, A. Schulz, A. Villinger, *Inorg. Chem.* **2014**, *53*, 3880–3892.
[44] C. Hering, J. Rothe, A. Schulz, A. Villinger, *Inorg. Chem.* **2013**, *52*, 7781–7790.

[45] A. Brückner, A. Hinz, J. B. Priebe, A. Schulz, A. Villinger, *Angew. Chem. Int. Ed.* **2015**, *54*, 7426–7430; *Angew. Chem.* **2015**, *127*, 7534–7538.
[46] C. Hering-Junghans, M. Thomas, A. Villinger, A. Schulz, *Chem. Eur. J.* **2015**, *21*, 6713–6717.
[47] J. Bresien, K. Faust, A. Schulz, A. Villinger, *Angew. Chem. Int. Ed.* **2015**, *54*, 6926–6930; *Angew. Chem.* **2015**, *127*, 7030–7034.
[48] J. Bresien, L. Eickhoff, A. Schulz, T. Suhrbier, A. Villinger, *Chem. A Eur. J.* **2019**, *25*, 16311–16319.
[49] J. Bresien, A. Schulz, M. Thomas, A. Villinger, *Eur. J. Inorg. Chem.* **2019**, *2019*, 1279–1287.
[50] A. Villinger, P. Mayer, A. Schulz, *Chem. Commun.* **2006**, 1236–1238.
[51] P. Mayer, A. Schulz, A. Villinger, *J. Organomet. Chem.* **2007**, *692*, 2839–2842.
[52] A. Schulz, P. Mayer, A. Villinger, *Inorg. Chem.* **2007**, *46*, 8316–22.
[53] A. Villinger, A. Westenkirchner, R. Wustrack, A. Schulz, *Inorg. Chem.* **2008**, *47*, 9140–2.
[54] R. Labbow, D. Michalik, F. Reiß, A. Schulz, A. Villinger, *Angew. Chem. Int. Ed.* **2016**, *55*, 7680–7684; *Angew. Chem.* **2016**, *128*, 7811–7815.
[55] R. B. Grossman, *The Art of Writing Reasonable Organic Reaction Mechanisms*, Springer Science + Business Media, New York, **2003**.
[56] I. Fleming, *Chem. Soc. Rev.* **1981**, *10*, 83.
[57] K. Bläsing, R. Labbow, D. Michalik, F. Reiß, A. Schulz, A. Villinger, S. Walker, *Chem. A Eur. J.* **2020**, *26*, 1640–1652.
[58] C. Hering, A. Schulz, A. Villinger, *Inorg. Chem.* **2013**, *52*, 5214–5225.
[59] A. Schulz, A. Villinger, *Chem. Eur. J.* **2010**, *16*, 7276–7281.
[60] P. Pyykkö, M. Atsumi, *Chem. Eur. J.* **2009**, *15*, 12770–12779.
[61] G. M. Sheldrick, *Acta Crystallogr. Sect. A* **2015**, *71*, 3–8.
[62] G. M. Sheldrick, *Acta Crystallogr. Sect. C* **2015**, *71*, 3–8.
[63] G. M. G. M. Sheldrick, *SADABS*, University of Göttingen, Germany, **2004**.

Manuscript received: March 22, 2021
Revised manuscript received: April 13, 2021
Accepted manuscript online: April 21, 2021